Spatial interpolation schemes for direct-hybrid computational aeroacoustics

CES Seminar

by

Ansgar Niemöller

Supervised by:

Michael Schlottke-Lakemper

Chair of Fluid Mechanics and Institute of Aerodynamics Aachen

Aachen, 2016

Erklärung

Hiermit versichere ich, dass ich diese Arbeit selbstständig mit der Unterstützung der Betreuer verfasst und keine anderen als die angegebenen Quellen und Hilfsmittel benutzt sowie Zitate kenntlich gemacht habe.

Statement of Originality

I hereby confirm that I have written this work independently with support by my supervisors and without contributions from any sources other than cited in the text and the acknowledgements.

Aachen, September 2016

Abstract

In the direct-hybrid method for computational aeroacoustics the acoustic field is computed by means of a coupled simulation. Acoustic source terms are extracted from the computed turbulent flow field and are then used in a pure acoustics simulation. For the spatial coupling an interpolation scheme is needed in order to allow the data transfer between non-conforming grids, which are used in both simulations. In this work the local Galerkin projection method for the spatial interpolation on joint hierarchical Cartesian grids is studied. It offers the advantageous properties to be conservative, optimal in the L_2 norm and allows an efficient implementation. Further, since the projection scheme is local, it is qualified for parallel execution in the context of large scale simulations. The implementation of the local Galerkin projection is validated and its capabilities are evaluated by computing the acoustic field generated by a pair of co-rotating vortices. The results show that an accurate source reconstruction on a much coarser grid is possible, which allows to significantly reduce the computational effort for the acoustics simulation.

Contents

1 Introduction

Aircraft-generated noise constitutes a severe issue in the neighborhood of airports and entry lanes. Besides fuel efficiency, noise reduction is a major topic in recent aircraft development, which is also enforced by political requirements [1]. In order to comply with this, the main sound generating components of an aircraft, i.e. the airframe and the engines, need to be accurately analyzed, thus allowing their optimization. For this purpose, sophisticated and highly parallel algorithms are necessary to predict the generated far-field noise [2].

In the research field of aeroacoustics, the sound which is generated by fluid motion is studied. The associated numerical area is called computational aeroacoustics (CAA). The most common approach to CAA are hybrid methods, in which the flow and the acoustic field are computed by separate means in a hybrid simulation. First, in a computational fluid dynamics (CFD) simulation the turbulent flow field is computed to obtain noise-generating source terms, which are then used for predicting the acoustic field. A well-known hybrid method is given by the combination of a large-eddy simulation (LES) and subsequently solving the acoustic perturbation equations (APE) [3, 4]. This separation allows large scale aeroacoustic simulations, whereas the computation of the source terms can usually be restricted to a small domain. The difference in scales between the turbulent flow and the acoustic field, as well as the use of different numerical solution schemes result in individual spatial resolution requirements for the two discretized problems. This will in general lead to non-conforming grids used in both simulations, which requires an interpolation scheme for the spatial coupling of both solvers.

In this work the spatial interpolation by local Galerkin projection for direct-hybrid CAA on hierarchical Cartesian grids is considered. In Sec. 2 the partial differential equations for predicting the acoustic field and the used numerical methods are described. Next, in Sec. 3 the Galerkin projection is introduced and its specialization for the given specifications is given. Simulation results are presented and analyzed in Sec. 4. Finally, Sec. 5 concludes this work with a summary of the findings.

2 Direct-hybrid computational aeroacoustics

Classical hybrid methods for CAA suffer from the limitation that in general two distinct simulation tools are used, which exchange coupling data for the computation of acoustic source terms via disk I/O. The direct-hybrid method [5] circumvents this issue since it couples the CFD and CAA solver in the same framework. This way both solvers can run simultaneously and exchange data in memory thus bypassing I/O restrictions.

In the following, the APE system and the numerical methods for the direct-hybrid CAA simulations used in this work are described.

2.1 Acoustic perturbation equations

The acoustic perturbation equations derived by Ewert and Schröder [6] allow the computation of sound propagation based on a flow simulation. The APE-4 system (Eq. 2.1-2.2) is used in this work, wherein the unknowns are the perturbed pressure p' and the perturbed velocity vector $\boldsymbol{u}'$.

$$\frac{\partial p'}{\partial t} + \bar{c}^2 \nabla \cdot \left(\bar{\rho} \boldsymbol{u}' + \bar{\boldsymbol{u}} \frac{p'}{\bar{c}^2} \right) = 0, \tag{2.1}$$

$$\frac{\partial \boldsymbol{u}'}{\partial t} + \nabla \left(\bar{\boldsymbol{u}} \cdot \boldsymbol{u}' \right) + \nabla \left(\frac{p'}{\bar{\rho}} \right) = \boldsymbol{q}_m. \tag{2.2}$$

Mean quantities and the source term $\boldsymbol{q}_m$ (Eq. 2.3), which is the linearized Lamb vector, stem from the flow simulation and thus need to be interpolated when using non-conforming grids.

$$\boldsymbol{q}_m = -\left(\boldsymbol{\omega} \times \boldsymbol{u} \right)' \approx -\left(\boldsymbol{\omega}' \times \bar{\boldsymbol{u}} + \bar{\boldsymbol{\omega}} \times \boldsymbol{u}' \right) \tag{2.3}$$

Further details on the APE-4 system can for instance be found in [7].

2.2 Numerical methods

The turbulent flow field is determined by means of a finite-volume (FV) based LES solver of second order accuracy that solves the unsteady compressible Navier Stokes equations. The solver is well established and has been used for various flow problems, particularities are for example found in [8, 9, 10, 11]. For solving the APE to obtain the acoustic field a nodal discontinuous Galerkin (DG) spectral element method is used

[12, 13]. Therein the exact solution on the cells of the computational grid, also referred to as elements, is approximated by polynomials. More specific, nodal basis functions, i.e. Lagrange polynomials with a collocation of integration and interpolation nodes are used. Discontinuities among neighboring elements at their common boundaries are allowed, thus a numerical flux is needed to describe the interactions between elements. The order of the DG method depends on the chosen polynomial degree. Details on the method and its implementation can be found in [14, 15]. The time integration is performed using a low-storage fourth-order Runge-Kutta scheme [16].

A joint hierarchical Cartesian grid is used for both solvers in the direct-hybrid method. The creation of such a grid can be outlined as follows. The starting point is an initial level zero square or cube which is bisected in each direction. This refinement process is recursively repeated until resolution requirements are fulfilled. In this manner parent-child relationships of cells on adjacent refinement levels and connections of neighboring cells on each level are formed. Regarding the coupled simulation both solvers may operate on different levels and cells of the same grid, thus a joint hierarchical Cartesian grid is formed. This leads to different possible mappings between cells that are used in both simulations, i.e. CFD and CAA. For the cases of one-to-one (Fig. 2.1a) or one-to-multiple (Fig. 2.1b) mappings of cells, a data transfer from the flow to the acoustics solver is trivial since the constant FV solution just needs to be copied to all nodes of the respective DG elements. However, given multiple-to-one mappings (Fig. 2.1c) a spatial interpolation scheme is required in order to interpolate the discontinuous piecewise constant fields on the cells of the flow solver with continuous polynomials on each DG element.

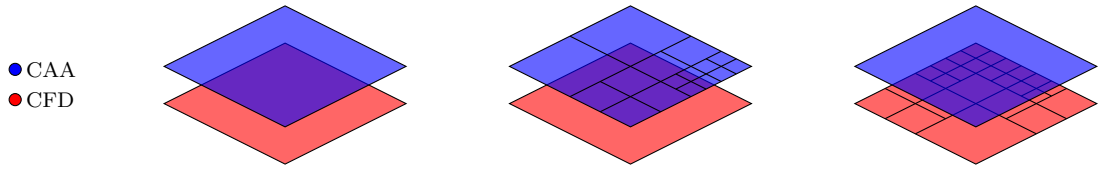

(a) one-to-one (b) one-to-multiple (c) multiple-to-one

Figure 2.1: Possible mappings of cells from the CFD to the CAA grid.

3 Spatial interpolation: local Galerkin projection

In the following, the local Galerkin projection method for spatial interpolation is presented [17]. Its general form as well as the specifications for the use on joint hierarchical Cartesian grids, following the derivation in [18], with an interpolation from a FV to a DG solver and aspects regarding the implementation are given.

In general the task is to interpolate a field q_D from the donor grid by q_T on the target grid, wherein both fields are allowed to be given in terms of different basis functions. The spatial interpolation is sought to be both conservative and optimal such that neither an unphysical behaviour nor large interpolation errors may occur. The Galerkin projection method considered here fulfills these two criteria.

3.1 General derivation

In the Galerkin projection method an interpolation is obtained by minimizing the L_2 error (Eq. 3.1) between the given donor field q_D and the interpolant or target field q_T with basis functions $\Phi_D^{(j)}, j \in \{1, \ldots, \mathcal{N}_D\}$ and $\Phi_T^{(i)}, i \in \{1, \ldots, \mathcal{N}_T\}$ respectively.

$$||q_D - q_T||_2 = \min_{q \in \mathcal{V}_T} ||q_D - q||_2 \tag{3.1}$$

This minimization is equivalent to: $\min_{q \in \mathcal{V}_T} ||q_D - q||_2^2$, i.e. minimizing the square of the L_2 norm. The interpolant $q = \sum_{k=1}^{\mathcal{N}_T} q^{(k)} \Phi_T^{(k)}$ fulfills this condition if the derivatives with respect to the coefficients $q^{(k)}$ of q vanish:

$$\frac{\partial}{\partial q^{(k)}} \int_\Omega (q_D - q)^2 \, dV = 0 \quad \forall k \in \{1, \ldots, \mathcal{N}_T\}. \tag{3.2}$$

Moving the derivative inside the integral and applying it yields Eq. 3.3. As the constant function 1 is contained in the basis it can directly be seen that this method is conservative.

$$\int_\Omega q_D \Phi_T^{(k)} dV = \int_\Omega q_T \Phi_T^{(k)} dV \quad \forall k \in \{1, ..., \mathcal{N}_T\} \tag{3.3}$$

With q_D and q_T expanded in its basis functions Eq. 3.3 can be written in matrix notation:

$$\mathbf{M}_T \mathbf{q}_T = \mathbf{M}_{TD} \mathbf{q}_D \quad \Rightarrow \quad \mathbf{q}_T = \mathbf{M}_T^{-1} \left(\mathbf{M}_{TD} \mathbf{q}_D \right), \tag{3.4}$$

with the so-called mass and mixed mass matrix $\mathbf{M}_T$ and $\mathbf{M}_{TD}$ respectively, with components given by integrals over products of basis functions:

$$(M_T)_{ij} = \int_\Omega \Phi_T^{(i)} \Phi_T^{(j)} dV, \qquad (M_{TD})_{ij} = \int_\Omega \Phi_T^{(i)} \Phi_D^{(j)} dV. \tag{3.5}$$

3.2 Local Galerkin projection in the direct-hybrid method

For the case of the considered direct-hybrid method with coupled FV-LES and DG-CAA simulation the local Galerkin projection for spatial interpolation can be specialized. On the FV grid there are only piecewise constant fields, thus there is only a single basis function $\Phi_D^{(1)} = 1$ on each donor cell. Further, as the interpolant is sought on each target element and with the properties of the joint hierarchical Cartesian grid, i.e. a child cell is always fully contained in its parent cell, it can be seen that each DG element can be considered individually. Since the donor field q_D is most likely discontinuous the evaluation of the integral expressions (Eq. 3.5) by Gaussian quadrature is performed on the intersection of the donor and target grid, which is the so-called supermesh [17]. The integral over the target element is therefore given by the sum of all integrals over donor cells contained in this element. With this the interpolant on a single target element (Eq. 3.4) can be written as:

$$\mathbf{q}_T = \mathbf{M}_T^{-1} \left(\sum_{k=1}^{S} q_{D_k} \mathbf{M}_{TD_k} \right), \tag{3.6}$$

with S the number of donor cells, q_{D_k} the value of the donor field on the k-th donor cell and $\mathbf{M}_{TD_k}$ the corresponding mixed mass matrix, which is just a vector given that there is only a single basis function on each donor cell. The vector entries are the basis functions of the target element integrated over the donor cell. Evaluation of the mass matrix using Gaussian quadrature yields that M_T is a diagonal matrix given by the Legendre-Gauss integration weights, thus its inversion is trivial.

3.3 Implementation

The local Galerkin projection for the considered direct-hybrid CAA on hierarchical Cartesian grids allows an efficient implementation that is outlined in the following. The main idea is to precompute all necessary information needed to apply the projection on all target elements and reuse it throughout the whole simulation. Thus, performing the Galerkin projection on a single element is only a sum of scalar-vector products with a

computational cost in the order of the number of target nodes times the number of donor cells of the element. Further, given that the considered spatial interpolation is local, a hybrid parallelization with OpenMP, when applying the projection to all elements, is straightforward.

The projection information to be computed are the vectors $\mathbf{M}_{TD_k}$ for each target polynomial degree, all relative refinement levels between donor cells and target elements and all possible donor cells on these levels. Using the properties of the hierarchical Cartesian grid, the possible combinations of donor cell levels and positions are uniquely defined. Here, computational cost can be reduced given that the projection vectors in 2D and 3D are just Cartesian products of the projection vectors in one dimension. This property is inherited from the polynomial basis. Further, the inverse of the mixed mass matrix given by the integration weights can be premultiplied to these projection vectors. Next, for each target element the information on the local donor cell configuration needs to be determined. In particular, for all the donor cells these are the relative refinement levels and the positions on the specific levels with respect to the target element. Applying the Galerkin projection with these information on one element basically consists of looking up the projection vectors corresponding to the donor cells, multiplying them with the associated values of the donor field and taking their sum.

4 Results

For the evaluation of the local Galerkin projection for the spatial interpolation in the direct-hybrid method the case of a pair of co-rotating vortices in 2D is considered [19]. Two point vortices, each with a constant circulation Γ, are placed in a quiescent medium. A co-rotation due to the reciprocally induced velocities can be observed and the acoustic field generated by this flow configuration is sought.

4.1 Computational setup

The computational domain, as pictured in Fig. 4.1a, is composed of a square CFD domain with a side length of $135r_0$ centered in the origin, which is enclosed by a square CAA domain of twice the size. The flow parameters are chosen according to [20], with the two point vortices located on a circle with radius r_0 around the origin (Fig. 4.1b). A high spatial resolution is required to accurately resolve the flow field, so grid refinement is used in order to obtain a resolution of $\Delta x_{min}/r_0 = 0.033$ in a circle of radius $5r_0$ in the center of the domain. The ratio of the maximum and minimum spatial step is given by $\Delta x_{max}/\Delta x_{min} = 16$. For the acoustic field it is generally necessary to accurately resolve the region of acoustic sources, but elsewhere, e.g. in the far-field, only the minimum wavelength significant in the considered problem needs to be resolved. For the DG-CAA different grids are used to analyze the influence of the spatial interpolation scheme.

4.2 Reference solution

To allow the validation and the evaluation of the capabilities of the Galerkin projection a reference simulation using conforming grids is carried out. With only one-to-one mappings between the two grids there is no need for a spatial interpolation. This reference setup is called $L13P1$, denoting the highest refinement level and the polynomial degree, here $p = 1$, used in the DG-CAA (Tab. 4.1). With $480,000$ DG elements there are about $1,9$ million degrees of freedom (DOF). In the center of the domain a spatial resolution of about 60 points per reference length r_0 is attained.

As can be seen in Fig. 4.2a, the computed acoustic field resembles a double spiral pattern corresponding to a rotating quadrupole source. The comparison along the positive x-axis at $t = 180$ (Fig. 4.2b) shows good agreement of the numerical and the analytical solution. Both solutions are scaled with their maximum value to allow the comparison

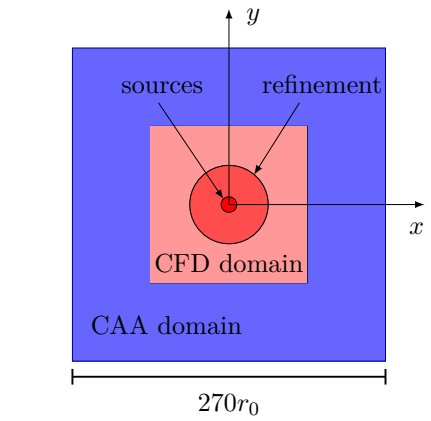

(a) Sketch of the computational domain.

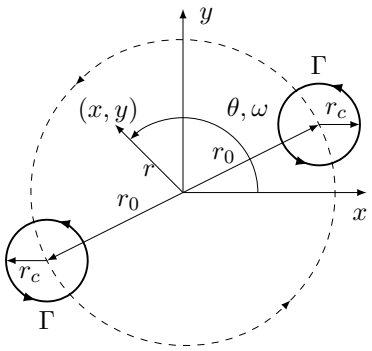

(b) Flow configuration.

Figure 4.1: Setup for the case of two co-rotating spinning vortices.

Setup	poly. deg.	$r_0/\overline{\Delta x_{min}}$	#elements	#DOF	mapping
L13P1	1	60.7	480,000	1,900,000	1 - 1
L11P3	3	30.3	30,000	480,000	16 - 1
L8P5	5	5.7	1,200	43,000	1024 - 1
L7P7	7	3.8	1,100	70,000	4096 - 1

Table 4.1: DG-CAA setups and the resulting mappings from LES to CAA.

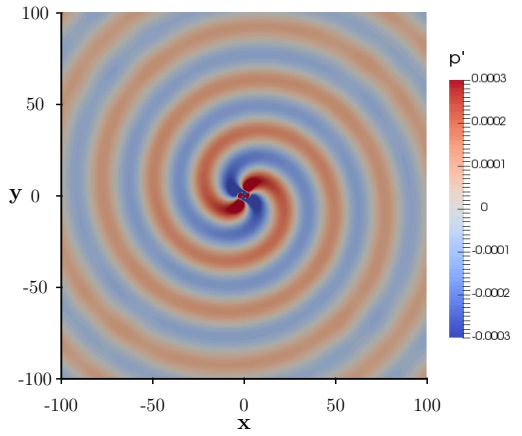

(a) Perturbed pressure p'.

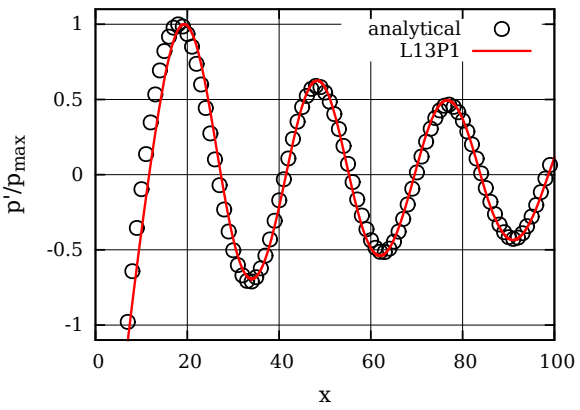

(b) Comparison with analytical solution along positive the x-axis.

Figure 4.2: Results of the $L13P1$ reference setup at $t = 180$.

despite differing amplitudes, which arise due to modeling assumptions concerning the vortices. In the following, this solution is used as a reference to allow the identification and quantification of interpolation errors.

4.3 Spatial interpolation

Starting from the $L13P1$ reference setup a first configuration that employs the spatial interpolation is obtained after reducing the overall refinement by two levels and increasing the polynomial degree to $p = 3$, thus named $L11P3$ (Tab. 4.1). This gives rise to a mapping of 16 cells from the LES to one cell of the CAA grid. The spatial resolution is effectively cut by half resulting in a quarter of the degrees of freedom in comparison to the reference. As shown in Fig. 4.3 the reference solution is perfectly matched by the solution obtained with the spatial interpolation. Thus, the conclusions can be drawn

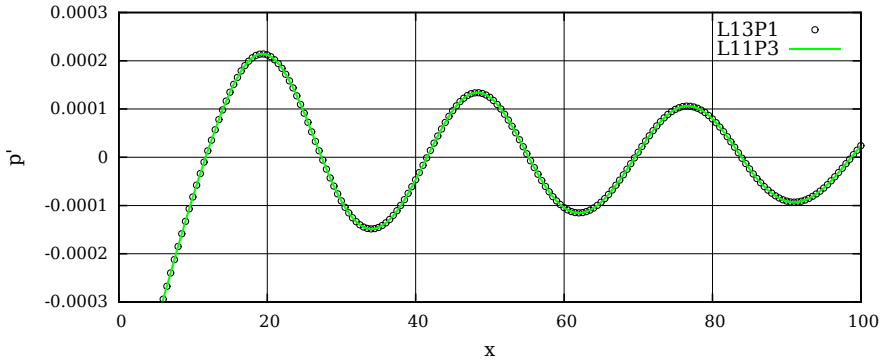

Figure 4.3: Perturbed pressure of the $L11P3$ setup along the positive x-axis.

that the Galerkin projection method works as intended and that its implementation is carried out correctly. Based on this, the capabilities and limits of the Galerkin projection for the acoustic source term reconstruction are now the subject of investigation. Next, a much coarser DG-CAA grid with polynomial degree $p = 5$ ($L8P5$) is used, with each 1024 FV-LES cells mapped to one DG-CAA element in the acoustic source region. The number of elements and corresponding to this the number of degrees of freedom is significantly reduced, resulting in a maximal spatial resolution that is only one-tenth of the one in the reference setup. However, as can be seen in Fig. 4.4 with all curves falling together there is no observable influence of the interpolation scheme on the quality of the solution. With less than 1/40 of the DOF compared to the reference setup and this huge amount of 1024 cells mapped to one element still the same solution is obtained. This shows that by employing the Galerkin projection method an accurate source reconstruction on a much coarser refinement level, while maintaining the solution accuracy, is possible. Spurious errors or disturbances are not present in the solution.

When further reducing the refinement level in the center of the domain and using $p = 7$ (L7P7), therefore reducing the spatial resolution in the acoustic source region, but

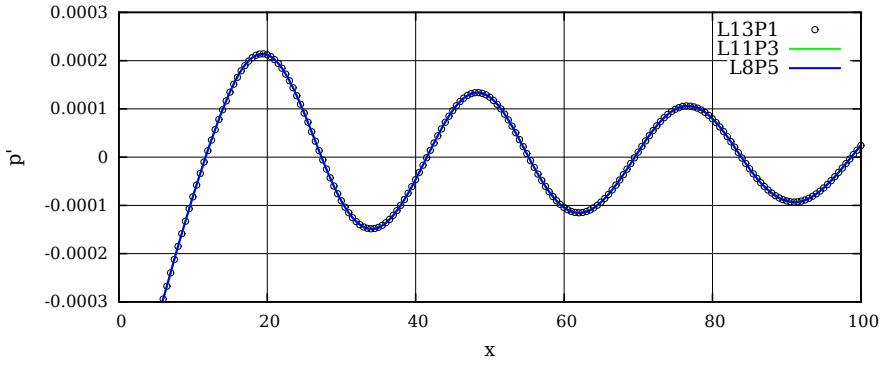

Figure 4.4: Perturbed pressure of the $L8P5$ setup along the positive x-axis.

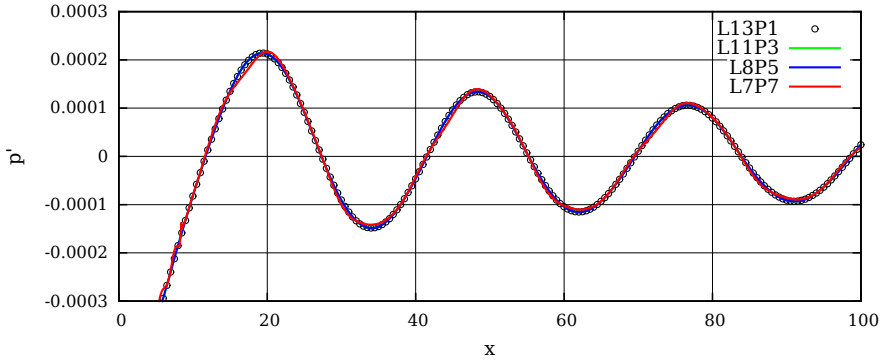

Figure 4.5: Perturbed pressure of the $L7P7$ setup along the positive x-axis.

effectively increasing the total number of DOF, first inaccuracies in the solution (Fig. 4.5) can be seen. With a maximal spatial resolution of merely 4 points per reference length r_0 it is obvious that the acoustic source terms on the CAA grid cannot be sufficiently represented anymore.

4.4 Runtime and efficiency

As shown previously, the use of the Galerkin projection allows to significantly reduce the number of DOF used in the DG-CAA without affecting the solution quality. The impact of this on the computational cost, i.e. the overall runtime for the direct-hybrid simulation, is pictured in Fig. 4.6a. Simulations for all setups were conducted using the same machine and each a parallel execution on 12 cores. Looking at the timings (Tab. 4.2), it is evident that the Galerkin projection allows a significant reduction of the computational cost. For the $L8P5$ case, with its much coarser grid in comparison to the $L13P1$ reference setup, a huge speedup of factor 17 is observable. The analysis of the relative runtimes (Fig. 4.6b) provides an impression which part of the direct-hybrid

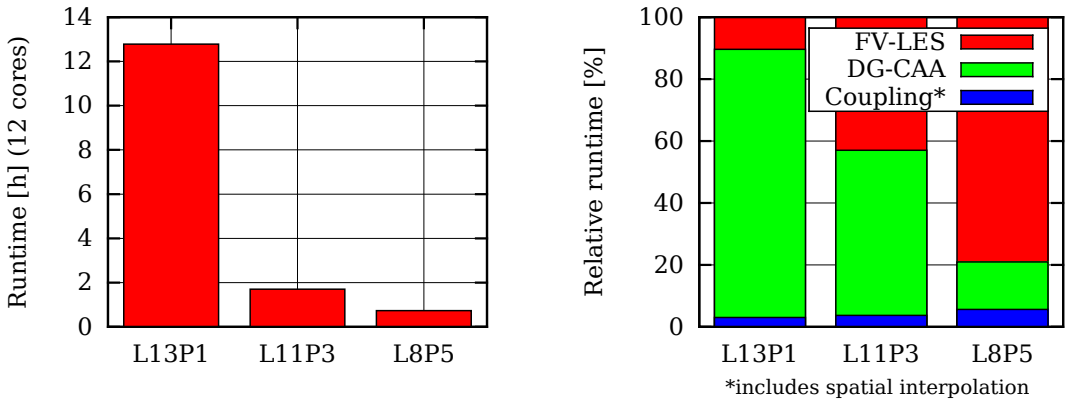

(a) Total runtimes.

(b) Relative runtimes.

Figure 4.6: Runtime comparison of different setups.

simulation is dominating the overall runtime. In the reference case the acoustic solver takes up nearly 90% of the total computational time. This ratio is decreased to about 15% in the $L8P5$ case, where about 80% runtime is spend for the flow simulation. The coupling with a maximum fraction of circa 5%, which includes the spatial interpolation, plays only a minor role in the overall computation. This reveals the efficiency of the Galerkin projection method since it does not introduce a considerable overhead to the computation. In summary it can be stated that speaking in terms of computational cost it is beneficial to use the coarsest possible DG-CAA grid with an appropriate higher polynomial degree. This approach seems to yield the maximum speedup and therefore can make large scale aeroacoustics simulations more feasible, since resource usage in terms of computing time is minimized.

Setup	Runtime [h]	FV-LES	DG-CAA	Coupling
L13P1	12.78	10.4%	86.6%	3.0%
L11P3	1.70	43.0%	53.3%	3.7%
L8P5	0.73	79.0%	15.4%	5.6%

Table 4.2: Runtimes of the different setups on 12 cores.

5 Conclusions

The local Galerkin projection method for the direct-hybrid method with a combined FV-LES and DG-CAA on hierarchical Cartesian grids has been presented. Its implementation was carried out and validated, as well as its capabilities were evaluated by means of the computation of the sound which is generated by a pair of co-rotating vortices. The results show that an accurate acoustic source reconstruction on a much coarser grid with an appropriate higher polynomial degree is possible without introducing spurious errors, while maintaining the solution accuracy. The use of the Galerkin projection thus allows a significant reduction of the computational cost, since non-conforming grids satisfying different resolution requirements for the flow and acoustics simulation can be employed. This is especially relevant for large scale aeroacoustic simulations in order to minimize resource usage and gain simulation results faster. In summary the Galerkin projection is a promising candidate for the spatial interpolation in direct-hybrid CAA. It is conservative as well as optimal in the L_2 norm, local and efficient. However, further research has to be conducted, for example regarding its applicability for simulating broadband noise or its capabilities in 3D. Other topics of interest are for instance the combination with a temporal interpolation [21] or the comparison to other spatial interpolation schemes.

Bibliography

[1] Directorate-General for Research and Innovation European Union, "Flightpath 2050: Europe's Vision for Aviation: Maintaining Global Leadership and Serving Society's Needs". Office for Official Publications of the European Communities, 2011.

[2] A. Niemöller, "Comparison of different methods for solving the acoustic perturbation equations", Bachelor's thesis, Chair of Fluid Mechanics and Institute of Aerodynamics Aachen, 2015.

[3] R. Ewert and W. Schröder, "On the simulation of trailing edge noise with a hybrid LES/APE method", *Journal of Sound and Vibration*, vol. 270, no. 3, pp. 509 – 524, 2004. 2002 I.M.A. Conference on Computational Aeroacoustics.

[4] S. R. Koh, W. Schröder, and M. Meinke, "Turbulence and heat excited noise sources in single and coaxial jets", *Journal of Sound and Vibration*, vol. 329, no. 7, pp. 786 – 803, 2010.

[5] M. Schlottke-Lakemper, M. Meinke, and W. Schröder, *A Hybrid Discontinuous Galerkin-Finite Volume Method for Computational Aeroacoustics*, vol. 132 of *Notes on Numerical Fluid Mechanics and Multidisciplinary Design*, pp. 743–753. 2016.

[6] R. Ewert and W. Schröder, "Acoustic perturbation equations based on flow decomposition via source filtering", *Journal of Computational Physics*, vol. 188, no. 2, pp. 365 – 398, 2003.

[7] M. Schlottke, H.-J. Cheng, A. Lintermann, M. Meinke, and W. Schröder, "A direct-hybrid method for computational aeroacoustics", *21st AIAA/CEAS Aeroacoustics Conference*, 2015.

[8] D. Hartmann, M. Meinke, and W. Schröder, "An adaptive multilevel multigrid formulation for Cartesian hierarchical grid methods", *Computers & Fluids*, vol. 37, no. 9, pp. 1103 – 1125, 2008.

[9] D. Hartmann, M. Meinke, and W. Schröder, "A strictly conservative Cartesian cut-cell method for compressible viscous flows on adaptive grids", *Computer Methods in Applied Mechanics and Engineering*, vol. 200, no. 9–12, pp. 1038 – 1052, 2011.

[10] L. Schneiders, D. Hartmann, M. Meinke, and W. Schröder, "An accurate moving boundary formulation in cut-cell methods", *Journal of Computational Physics*, vol. 235, pp. 786 – 809, 2013.

[11] C. Günther, M. Meinke, and W. Schröder, "A flexible level-set approach for tracking multiple interacting interfaces in embedded boundary methods", *Computers & Fluids*, vol. 102, pp. 182 – 202, 2014.

[12] J. S. Hesthaven and T. Warburton, *Nodal Discontinuous Galerkin Methods*. Texts in Applied Mathematics, Springer, 2008.

[13] G. Gassner, "Discontinuous-Galerkin-Verfahren", *Institut für Aerodynamik und Gasdynamik der Universität Stuttgart*, 2013.

[14] D. A. Kopriva, *Implementing Spectral Methods for Partial Differential Equations*. Springer, 2009.

[15] F. Hindenlang, G. Gassner, C. Altmann, A. Beck, M. Staudenmaier, and C.-D. Munz, "Explicit discontinuous Galerkin methods for unsteady problems", *Computers & Fluids*, vol. 61, pp. 86 – 93, 2012.

[16] M. H. Carpenter and C. Kennedy, "Fourth-order 2N-storage Runge-Kutta schemes", *NASA Report TM 109112, NASA Langley Research Center*, 1994.

[17] P. Farrell and J. Maddison, "Conservative interpolation between volume meshes by local Galerkin projection", *Computer Methods in Applied Mechanics and Engineering*, vol. 200, no. 1–4, pp. 89 – 100, 2011.

[18] A. Marwege, "Conservative Galerkin projection for hybrid computational aeroacoustics on hierarchical Cartesian grids", Bachelor's thesis, Chair of Fluid Mechanics and Institute of Aerodynamics Aachen, 2015.

[19] D. J. Lee and S. O. Koo, "Numerical study of sound generation due to a spinning vortex pair", *AIAA Journal*, vol. 33, pp. 20–26, Jan. 1995.

[20] C. Bogey, C. Bailly, and D. Juvé, "Computation of Flow Noise Using Source Terms in Linearized Euler's Equations", *AIAA J.*, vol. 40, no. 2, pp. 235–243, 2002.

[21] G. Geiser, D. Marinc, and W. Schröder, "Comparison of source reconstruction methods for hybrid aeroacoustic predictions", *International journal of aeroacoustics*, vol. 12, no. 7/8, pp. 639–662, 2013.